NEW MEXICO TECH
SCIENCE • ENGINEERING • RESEARCH • UNIVERSITY

Senate Bill

Short Title: Imece 2019 conference

Agency, Agent, or Individual Proposing: Douglas MacNinch

Requested Date of Resolution: 22 day of 2019

Proposing Individuals' Information:

Name 1: Douglas MacNinch **Title**: _____

Phone: 505-228-5633 Email: douglas.macninch@student.nmt.edu Campus Box: _____

Student/Non-Student: Student Signature: _____

To the Proposing Agency, Agent, or Individual:

Please attach a typewritten explanation of your needs and/or concerns in double-spaced 12-point format, placing a page number and title on the top of each page. Include all information necessary and pertinent to your argument. State exactly what action you would like the Senate to consider taking and by when you must have a decision. Please take in to consideration that the Senate meets approximately once every two weeks while classes are in session – a schedule is available from the SGA Secretary.

Please see the Manual for Drafting Bills to help fill this page out; it includes explanations and examples for each field. If you have any further questions, please contact the SA Vice President.

OFFICE OF THE VICE PRESIDENT USE ONLY

Date Presented to the Vice President: 10/21/19 Initials of Receipt by Vice President: DS

Session of the Senate: (X) Fall ( ) Spring/Summer of the calendar year 2019

Amount Approved: _____

OFFICE OF THE PRESIDENT USE ONLY

Presidential Signature: _____ Date: _____

IMECE 2019 Conference

To whom it may concern,

My name is Douglas MacNinch and I am a Senior Mechanical Engineering student here at Tech graduating this December. As part of the Mechanical Engineering curriculum, I am part of the In Orbit Structural Health Monitoring (IOSHM) design team. Our team has written a paper that will be published in the ASME database and also stored in the archives at the Library of Congress. This paper details our work on this project from conception to completion.

As part of the publication process the lead author is required to attend the conference and give a ten minute presentation. If our team is not represented at the conference, our paper will not be published. I am the lead author, and so I am requesting funding from the SGA for travel, lodging, and food while I attend the conference from November 11th to November 13th of this year.

To aid in you decision, I will be attaching a copy of our paper along with the required forms. The conference is less than three weeks away, so I would like to know your decision as soon as possible so that I can make other arrangements as necessary.

Thank you for your consideration,

Douglas MacNinch

Proceedings of the ASME 2019
International Mechanical Engineering Congress and Exposition
IMECE2019
November 11-14, 2019, Salt Lake City, UT, USA

IMECE2019-12093

MECHANICAL DESIGN AND DEVELOPMENT OF A PAYLOAD FOR STRUCTURAL HEALTH MONITORING EXPERIMENTS ON THE INTERNATIONAL SPACE STATION

Douglas MacNinch, Daniel Pacheco, Arjun Tandon, Carl Bancroft, Isaac Flores, Matthew Rue, Andrei Zagrai

New Mexico Institute of Mining & Technology (NMT)
Socorro, New Mexico, United States

ABSTRACT

This contribution reports design and development of a payload for structural health monitoring (SHM) experiments on the International Space Station (ISS). The payload was designed to operate in low earth orbit (LEO) environment and fit specifications of the Materials International Space Station Experiment (MISSE) module. In particular, LEO environmental factors such as a strong vacuum, thermal variations from -18°C to 60°C [1], and background radiation were considered. The payload is a rectangular multi-leveled structure which houses several SHM experiments, active sensors self-assessment, and electronic hardware with data storage and retrieval capabilities. SHM experiments include guided wave propagation in a metallic structure, monitoring of an imitated crack, assessment of a bolted joint, investigation of structural vibration via electromechanical impedance method, and acoustic emission monitoring. In addition, piezoelectric sensor self-assessment is realised using impedance diagnostics. It is anticipated that the payload will operate for one year in LEO and provide insights on the effect of space environment on SHM of future space vehicles during long-duration flights. This contribution focuses on mechanical design of the payload to support SHM experiment. Specific arrangement of payload elements and implementation of boundary conditions for SHM experiments are reported. Theoretical calculations and examples of SHM experimental data obtained in laboratory tests are presented and discussed in light of expected variations due to LEO environment. Measures to protect SHM hardware from harsh space environment are presented. Perspective applications of SHM as an integral component of future space systems are discussed.

Keywords: Mechanical Design, Experimental Test Plate, Low Earth Orbit, Structural Health Monitoring, Finite Element Analysis, Atomic Oxygen, Solar Radiation, Static Loading, Thermal Stress, International Space Station.

1. INTRODUCTION

As technology progresses and the world reaches further out into space, the need for safe and reliable space structures will increase exponentially. In the world today, there are thirteen countries with space programs, and in the United States alone, there are more than thirty privately-owned space vehicle manufacturers. At this very moment, there are roughly 4,900 satellites, two space stations with six humans orbiting our planet [24]. As space becomes increasingly commercialized and more people are able to visit; the need for safety will take precedence.

Structural health monitoring (SHM), is the process by which the structural integrity of an object is evaluated using a system of structurally integrated sensors and actuators. SHM is among one of the critical technologies to enable safe and reliable space systems. One of the first SHM studies focused on the use of Bragg-grating fiber optic sensors that were placed on

[1] Douglas MacNinch: douglas.macninch@student.nmt.edu
[2] Daniel Pacheco, Arjun Tandon, Carl Bancroft, Isaac Flores, Matthew Rue, Andrei Zagrai

the liquid hydrogen fuel tank of the NASA/ McDonnell Douglas Delta DC-XA reusable rocket [2]. Fiber optic technology for SHM on space vehicles has been considered by many researchers [3,4,5,6], however, a disadvantage of the fiber optic SHM is that it is passive technology and is not able to interrogate a structure on demand. For this reason, there has been considerable interest in embedded ultrasonic sensors [7], which utilize small and unobtrusive piezoelectric actuators to launch guided waves into aerospace structures while similarly small unobtrusive piezoelectric sensors detect changes in elastic wave propagation or the reflection signals caused by material damage [8,9]. Several applications of embedded ultrasonic sensor SHM on space structures have been reported, including rocket engines [10], TPS [11], plate structures [12] and bolted joints [13]. Of particular interest to this paper, were the active ultrasonic experiments. In 2011, the New Mexico Tech, In Orbit Structural Health Monitoring (IOSHM) team demonstrated electro-mechanical impedance monitoring of bolted joints while on the SL5 sub-orbital flight [14]. Then in 2013, the condition of a payload was monitored in real time during the SL8 sub-orbital flight, in which experiments included detection of a crack, loosely bolted joints, recovering dispersive characteristics of a metallic plate and acoustic emission monitoring [15]. Unfortunately, sub-orbital fights only expose a payload to the space environment for a short time whereas a long-term exposure to the space environment is more desirable.

This paper discusses the design and development of a payload that will house experiments enabling active SHM in the low earth orbit (LEO) environment aboard the International Space Station (ISS). The practical applications of SHM are limitless, and the methods used in this paper could potentially detect material abnormalities such as corrosion or oxidation, physical damage such as dents, dings, scratches or holes and manufacturing defects such as loose or missing bolts or rivets.

2. MISSION PROFILE AND SPACE ENVIRONMENT

The design of this payload included accounting for several environmental factors in the LEO such as atomic oxygen (AO) corrosion, radiation, and vacuum, which are discussed in the following sections.

2.1.Mission Profile

It is anticipated that the payload for long term SHM in the space environment will be a part of the 12th installment of the Materials International Space Station Experiment (MISSE-12). As part of the MISSE-12 directive, the payload will spend a minimum of 12 months aboard the ISS in low earth orbit. The ISS orbits the Earth once every 92 minutes at an average orbital range of 400-km [1]. The payload is planned to have a WAKE orientation aboard the MISSE-12, which is characterized by minimal exposure to atomic oxygen and a view over the ISS structure. The main concern is the hazards brought from radiation and the vacuum of LEO. While in orbit, the payload will conduct a series of SHM experiments. Ultimately the purpose is to demonstrate the feasibility of a structural health monitoring system for future use in long term space missions.

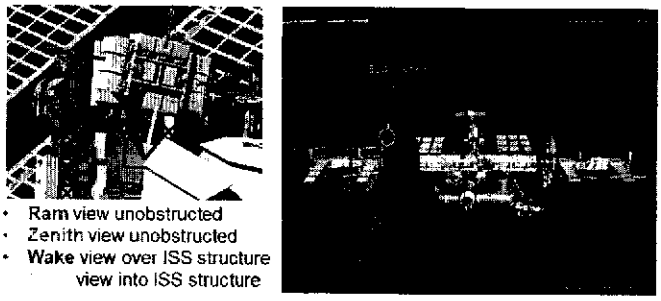

FIGURE 1: MISSE-12 ORIENTATION AND LOCATION ON THE ISS [9].

2.2. Thermal Fatigue and a Cycling Thermal Gradient

While the payload is operating on the ISS, it will experience radiation and extreme cold while it is cast in a shadow, either due to Earth's shadow or the ISS [1]. It will also be exposed to harsh sunlight as the Sun's radiation will be emitting heat on the payload. The payload will only be experiencing thermal radiation as the vacuum environment makes conduction and convection non-existent [17]. Thermal radiation will consist of Solar, albedo, infrared emitted by Earth, and infrared emitted by the ISS [1]. The thermal gradient cycles from -18°C to 60°C and as the payload orbits the Earth, the payload will be undergoing thermal expansion and contraction from the various temperature variations. This will result in thermal fatigue of the payload and could cause micro-cracks on the surface of the payload.

2.3. Vacuum Environment and Alteration of Properties

The LEO environment has a high vacuum ranging from 10^{-6} to 10^{-9} Torr. This vacuum pressure causes outgassing which occurs when the vapor pressure of a material is higher than the pressure of the vacuum. This outgassing can condense on optical sensors, solar panels, and other sensitive equipment which can cause complications. This outgassing can also cause deformities of the payload and could skew the data collection. To alleviate this problem, Aluminum 6061-T6 was chosen as the primary material as it is approved by NASA to have low outgassing.

2.4. Radiation and Electrostatic Environment

The Sun, cosmic rays and radiation belts around the Earth are the primary sources of radiation which the ISS and the payload will experience. A photon flux of 0.1 eV to 1 keV [1] can be observed in this environment due to solar ultraviolet radiation. Excessive radiation exposure can cause corruption of the data collection through malfunction of electronic equipment within the payload. Considering this, the 6061-T6 aluminum which the payload is fabricated from serves as a barrier to radiation.

Electrostatic discharge occurs when the surface of a body is charged by radiation, magnetic fields or high energy electrons. Ionospheric plasma is the most abundant source of natural charge. It is formed when oxygen and nitrogen are ionized by solar radiation which then ionizes to create low

energy, high-density electrons. An ionosphere discharge of 0.1 eV will be observed. This discharge can cause malfunctions of electrical equipment present in the payload.

2.5. Micrometeoroid and Orbital Debris Collisions

A critical concern for the project was the effect of micrometeoroid and orbital debris (MMOD) collisions. A micrometeoroid is any object in the LEO environment that has an average mass of 1 gram and an average velocity of 10 km/s [1]. Using the kinetic energy equation, each of these objects has an average kinetic energy of 50 kJ/m^2. Understandably, MMOD collisions can be devastating in and of themselves. Compounding to the problem is the domino-like Kessler Effect. Due to the presence of space junk, the Kessler effect states that a single collision can instigate a cascade of subsequent collisions, and the combined energy of these collisions pose the possibility to damage the payload severely. For that reason, the payload will be mounted in a position that minimizes possibilities of orbital debris damage.

2.6. Atomic Oxygen Corrosion

Atomic oxygen (AO) is the unstable and highly reactive form of oxygen. When diatomic oxygen (O_2) enters LEO, the ionosphere and radiative environments cause electron shearing which subsequently causes separation of the oxygen molecules; in their natural state, oxygen molecules have a charge of -2, and the separation of an oxygen pair causes a charge imbalance, which results in highly reactive AO. With the high charge densities, AO exists freely and abundantly in LEO. With flux concentrations of up to 3.33 x 10^{23} atoms/cm^2 (8.842 g/cm^2) [1], AO combines with aluminum atoms and the unusable product, Al_2O_3, drifts away, leaving behind a cavity in the structure, i.e., corrosion caused by AO. With this in mind, the payload uses a thick shielding layer of aluminum to reduce the effects of AO corrosion on the experiments.

2.7. Passive Vibration Environment

The ISS undergoes microgravity vibration due to transient or non-transient origins. These vibrations have frequencies ranging from 10^{-5} to 1 Hz. At low frequencies, the causes can be traced to atmospheric drag, gravity gradient due to the Earth, and vibrations due to the motions of the ISS crew. The higher frequencies can be traced to mechanical components, impacts, and thruster firings [12]. These vibrations would need to be considered as the payload will be conducting experiments related to guided wave and electromechanical impedances. The position of the payload would also need to be considered as the range of frequencies vary depending on where the non-transient vibrations are occurring.

3. SHM EXPERIMENTS ON ISS

The payload will house a total of seven experiments which are as follows:

1) Imitated Crack Detection
2) Detection of Loose Bolts
3) Acoustic Emission
4) Electro-mechanical impedance measurement of the piezoelectric sensor to obtain its electro-mechanical dynamic characteristics
5) Electro-mechanical impedance measurement of the plate structure to study its vibration characteristics
6) Measurements of structural dispersion curves
7) Passive piezoelectric transducer degradation

The payload will house an MD7-Pro Digital SHM system which is comprised of acquisition and accumulation nodes connected to a distributed piezoelectric sensor array. The acquisition node will transmit an acquired ultrasonic signals, and the accumulation node will act as the CPU for the system and store data. An actuator will excite the plate while distributed sensors receive the signal. Experiments 1, 2, 3 and 6 will be conducted on aluminum test plate one and require three sensors and one actuator. Experiment 5 will be on aluminum test plate two with one active sensor which will serve as both actuator and sensor. The setup of experiments on two plates in the payload can be seen in Figure 2. Experiment 6 includes a measurement of electro-mechanical dynamic responses of free piezoelectric sensor positioned between two experimental plates as also illustrated in Figure 2. Experiment 7 will be located on the top plate in order for the camera attached to the MISSE-12 compartment to capture its degradation in real time.

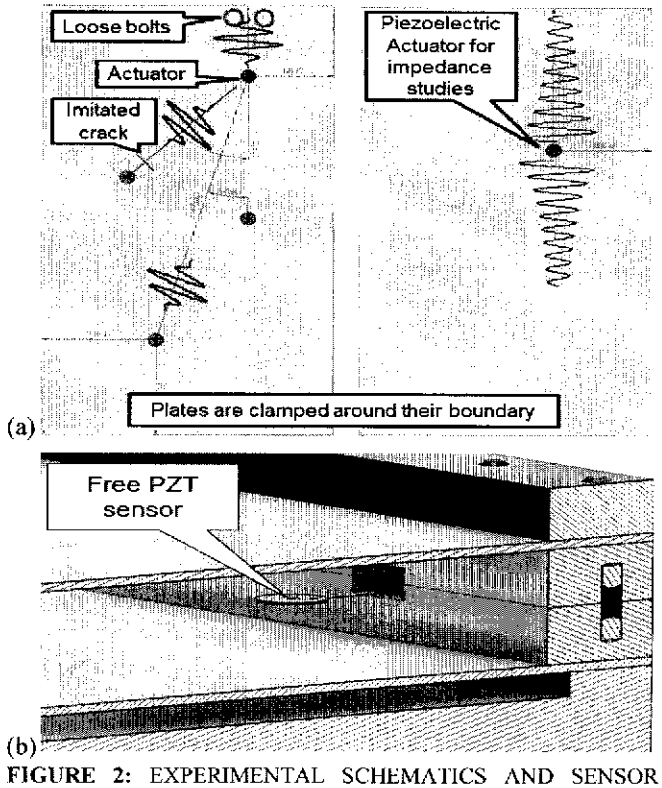

FIGURE 2: EXPERIMENTAL SCHEMATICS AND SENSOR DISTRIBUTION FOR (a) PLATE 1, PLATE 2 (b) AND FREE SENSOR BETWEEN PLATES.

4. PAYLOAD MECHANICAL DESIGN

The payload was designed in accordance with the requirements of the payload integrator, Alpha Space Test & Research Alliance, LLC. A set of geometrical dimensions restricts the design, requirement not to have loose parts, and must be self-sufficient and able to survive for up to one year in the LEO environment. The payload was designed as a rectangular box with dimensions of 152.4-mm by 266.7-mm by 63.5-mm or a volume of 2.581-mm^6. The material chosen was 6061-T6 Aluminum, a material that many current space vehicles are made from and which is NASA-approved. Within the payload, two rectangular test plates with adhered piezoelectric sensors are located. The lower portion of the payload contains the data acquisition system and related electronic components responsible for sensor operation and data collection. These electronics need protection from solar radiation and kept at temperatures no more than 65°C to prevent data corruption and data loss, thus leading to the inclusion of a 1-cm thick radiation shielding layer and the incorporation of a heat sink to the electronics base. A series of wires power the sensors and transfer the data back into the electronics, along with a pair of channels integrated along each of the 127-mm sides of the middle frames, test plates and compartment frame. The final design element would be the physical connection and the power connection points to the MISSE platform.

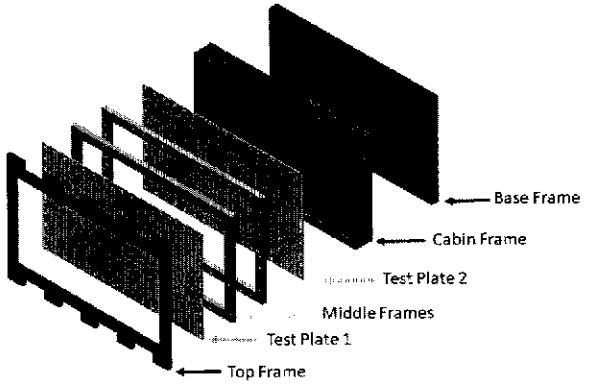

FIGURE 3: EXPLODED (STRUCTURAL ONLY) VIEW OF PAYLOAD DESIGN WITH EACH COMPONENT LABELED.

4.1. Top Frame

The design of the top frame was crucial to the survivability of the payload. The top frames main operation is to attach to the MISSE platform. This required the design to have five mounting tabs located along each of its 266.7-mm sides. The 6.4-mm thickness provides structural rigidity to the frame while also providing ample thread engagement space for bolting the first test plate and middle frame together. While referencing to Figure 3, the top frame design incorporates ten 25.4-mm by 12.7-mm mounting tabs evenly spaced along the 266.7-mm side of the payload. Each tab has a centered 5-mm hole in which to bolt the payload to the MISSE platform securely. This frame is 7-mm tall and with the mounting tabs has an overall width of 177.8-mm. Centered along this 177.8-mm side is a single piezoelectric sensor which will be used to study how the LEO environment affects the sensors themselves.

4.2. First Test Plate

Below the top frame and between one of the middle plates is the first test plate which can be seen in Figure 3 as test plate 1. This plate is made from 1.016-mm thick 6061 T6 aluminum and will incorporate three piezoelectric sensors and one piezoelectric actuator. These sensors will perform three separate experiments which include the imitated crack, loose bolt detection, dispersion and the acoustic emissions experiments.

4.3. Middle Plates

The middle frames referenced in Figure 4 and Figure 5 were designed to be interchangeable as a mounting companion to the top frame and first test plate or the second test plate and the compartment frame. The middle frames were designed to touch back-to-back but not to attach to one another. This design essentially creates two test plate assemblies that bolt together to form a single payload. The idea of mounting the middle frames back to back allows the forty-four each mounting bolts to be placed head to head which is depicted in Figure 4. This makes it impossible for any loose bolts to escape from the payload during any portion of its trip in LEO. Each middle frame is 7-mm thick and has two wire channels centered along each of the 152.4-mm sides. The wire channels were designed to fit in the center of the middle frames between the mounting holes as to not interfere with the fixed-fixed boundary conditions. The middle frames are bolted to either the top frame or cabin frame with forty-four each M3 x 5-mm Mil-Spec black oxide cap bolts. The top frame and the compartment frame will then have forty-four each 3-mm helicoil inserts to protect the aluminum payload from the threading and unthreading of the steel bolts.

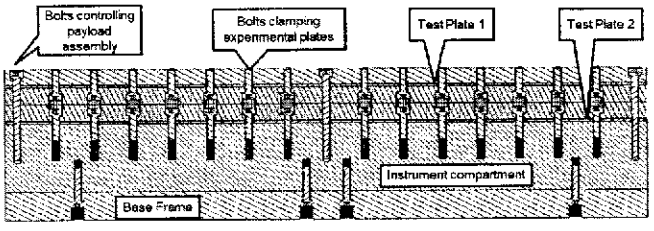

FIGURE 4: HEAD TO HEAD BOLTING PATTERN

4.4. Second Test Plate

The second test plate, which is between the second middle frame and the compartment frame is physically identical to the first test plate. However, this plate will house the Electromechanical Impedance experiment. This experiment will test the vibration characteristics of the plate.

4.5. Cabin Compartment Frame

The next component is the compartment frame which provides a housing for the electronic components. This portion of the payload is critical to protecting the electronics housed within. The four sides of the compartment frame are 12.7-mm

thick and are designed to protect the electronics from solar radiation. Along one of the 127-mm sides is a 10-mm diameter hole which was designed to allow a power source from the MISSE platform to enter the payload and power the electronics within. The top side of the compartment frame was designed with a 3-mm depression to allow room for the array of sensors to be secured to the bottom of, test plate two. The compartment frame was also designed with two wire channels that match up with the channels designed into the middle frames and test plates.

4.6. Base Frame

Attaching to the bottom of the compartment frame is the base frame. The base frame was designed to bolt to the bottom of the compartment frame using twelve M3 x 8-mm Mil-Spec black oxide steel bolts. Each of the four electronic components will be secured to the top side of the compartment frame within the inner dimensions of the compartment frame walls. Each component is secured by a thin aluminum bracket connected to the base frame with four each M3 x 3-mm Mil-Spec black oxide steel screws and will also be adhered to the base with a thermally conductive adhesive paste. On the bottom side of the base frame is a set of forty-three 1.59-mm wide by 5-mm tall grooves which create a heat sink that was designed to keep the electronics within their working temperature range.

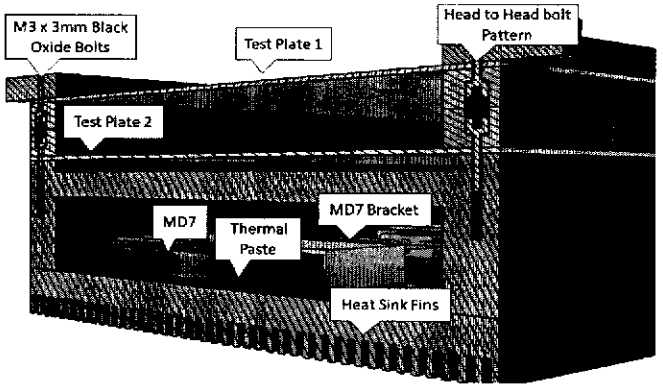

FIGURE 5: CUTAWAY SHORTVIEW DEPICTING HEAT SINK FINS.

4.7. Radiative Fins

Regulating the temperature of the payload is crucial to ensuring the success of the project. After contacting the manufacturer of the MD7, the optimal operating temperature was discovered to be 40 °C to 65 °C. With radiation being the only means of heat transfer in space, the team decided to add radiative heat fins to the bottom of the electronic housing base. At the time of the design, the thermal gradient of the payload was expected to be from -120 °C to 120 °C and as such the heat sink was designed for these conditions. In order to optimize the number of fins needed a MATLAB script was written to calculate the radiative heat transfer rate from the electronic base and through the heat sink. This process utilized the equations given in [23]. Figure 6 illustrates the optimization of the heat sink where the number of fins were chosen as the point after the zero-crossing in the heat transfer difference. At the output of this optimization, forty-three fins of 0.1994cm thickness were chosen.

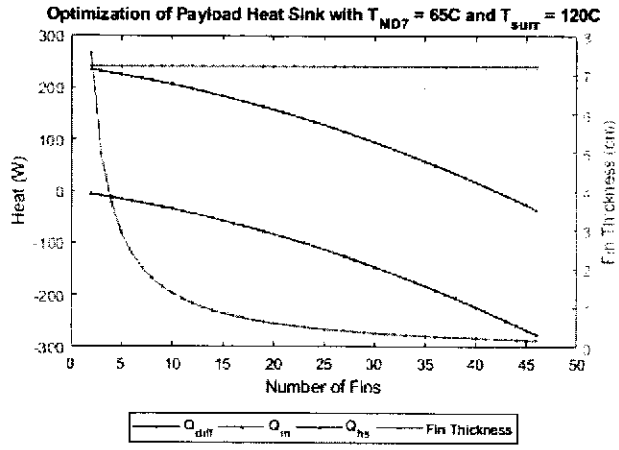

(a)

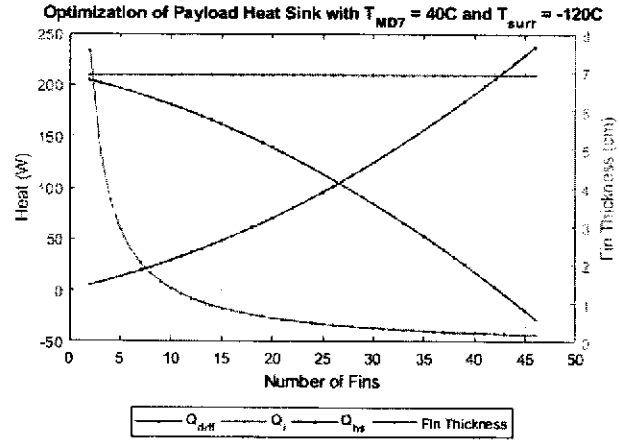

(b)

FIGURE 6: OPTIMIZATION OF THE PAYLOAD'S HEAT SINK AT (a) MAXIMUM ELECTRONIC AND LEO TEMPERATURE AND (b) MINIMUM ELECTRONIC AND LEO TEMPERATURE

4.8. Other Design Considerations

The design went through many iterations as the team progressed toward the final design. One of the most considered variables throughout the design processes were the boundary conditions for the experimental test plates. The boundary conditions for each of the test plates are critical when establishing baseline eigenfrequencies. The first iteration incorporated a simply supported knife-edged design. This design consisted of a total of eight knife-edged pieces of steel that were designed to fit within a groove cut around the edges of the middle frames, top frame, and compartment frame. These knife edges would face one another, top and bottom, and clamp the test plates between them. This design was found to be unstable, hard to manufacture and not capable of creating a repeatable boundary condition. The second iteration was a simply supported clamped roller design. This design was similar to the knife-edged design in that rolled pieces of steel

would rest in grooves on either side of the middle frame to top frame connection or the middle frame to cabin frame connection. The test plates would then be clamped between. This design was also found to have inconsistent boundary conditions which caused uneven stress distribution due to variations in contact pressure that the steel rods were exerting on the aluminum test plates. The design option found to be most effective for the design criteria was the fixed-fixed boundary condition. The fixed-fixed condition was incorporated by the use of forty-four M3 x 3-mm black oxide bolts, fourteen on each of the two 266.7-mm sides and eight each on the two 152.4-mm sides. This boundary condition is the most consistent and easiest to manufacture compared to the other design options.

5. FINITE ELEMENT MODELING AND ANALYSIS

5.1. Static Loading Environment

Static loading analysis consisted of considering static loading conditions that the payload would experience during its deployment. From Falcon 9 Rocket data, Figure 7, a loading environment was developed using COMSOL Multiphysics 5.3. A simplified payload model was subjected to three different loading orientations, refer to Figure 8, to evaluate potentially compromising stresses. Longitudinally, the payload was subjected to gravitational accelerations ranging from -4Gs to 9Gs; axially, gravitational accelerations ranged from -3Gs to 3Gs (1G equates to 9.81 m/s^2).

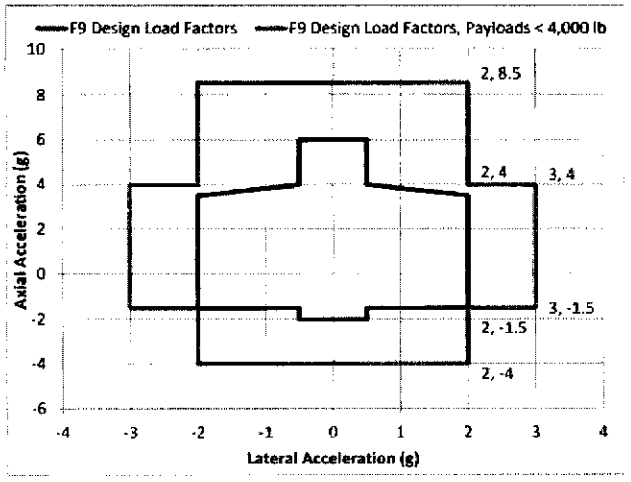

FIGURE 7: FALCON 9 AXIAL AND LATERAL LOADING DATA. [19]

5.2. Static Loading: Experimental Test Plates

With variable orientations for the payload, the critical components to evaluate were the experimental test plates: with a thickness of 1.016-mm, the accelerations and subsequent static loads experienced could potentially damage the test plates via plastic deformation and compromise the entirety of the experiments. A finite element (FE) model was constructed in COMSOL Multiphysics 5.3 to simulate the forces a plate would undergo. The CAD model of the plate was loaded into COMSOL, which proceeded to create a CAD-kernel file. 6061-T6 aluminum was selected as the material, with a density of 2.7g/cm^3, Young's Modulus of 68.9 GPa, tensile strength ranging from 124 MPa to 290 MPa and Poisson's ratio of 0.33. Fixed boundary conditions were applied at the four walls, as well as the interior of each hole; these conditions represent the physical clamping that an experimental test plate experiences in the payload. Gravitational loads were applied in the three loading configurations at the maximum acceleration (i.e., 9Gs). At this condition, the plate is most susceptible to failure or deformation; the paramount configuration of analysis is depicted below in Figure 8; arrows depict loads of different orientation.

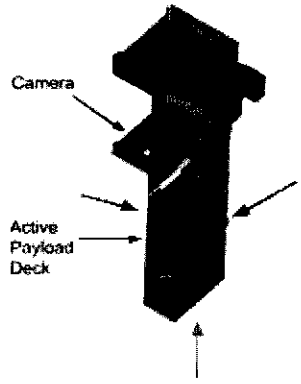

FIGURE 8: ORIENTATION OF PAYLOAD [23].

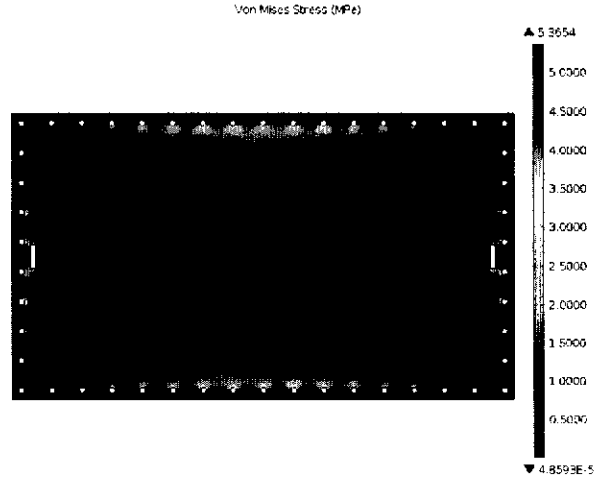

FIGURE 9: STRESS ON TEST PLATE FROM FE ANALYSIS WITH ACCELERATION APPLIED NORMAL TO THE SURFACE.

Next, an FE model was constructed with a finer mesh setting (element sizes ranging from 2.67-mm to 21.3-mm at a maximum growth rate of 1.45, resolution of 0.6, and a curvature factor of 0.5); the convergence of the solutions determined the element size and meshing factors: at smaller mesh sizes, divergence in the FE studies grew. From the FE studies, the respective safety factors for the three orientations were found by the ratio of the maximum stress the plate

experienced to the Young's Modulus (i.e., 68.9 GPa for Aluminum 6061): these factors are 1.54M for long-side orientation, 872,000 for short-side orientation, and 12,800 for surface orientations as shown in Figure 9. While it may seem that these values are extraordinarily high, due to the nature of the mission, these parameters fall safely in the operational window (i.e., overdesigning is not a problem).

5.3. Static Loading: Simplified Payload Geometry

A simplified payload model was developed with COMSOL using five blocks that were modeled from the basic dimensions of the payload such as the width, depth, and height. The payload was simplified because COMSOL attempts to create infinitesimally small elements compared to the average elements, which overconstrained the COMSOL models. The simplified model prevented the FE analysis from converging to improper values borne out of over-constrained geometries. The first block was the payload itself having dimensions of 15.24-cm by 6.35-cm by 26.67-cm and with the center of the block positioned 3.175-cm in the Y-direction and 0-cm in the other two directions. The next block was the cavity for the electronics which had the dimensions of 12.7-cm by 1.9812-cm by 24.13-cm and positioned 4.1656-cm in the Y-direction and 0-cm in the X-direction and Z-direction. The first block was subtracted by the second block to make the cavity of the electronics. The third block had the dimensions of 12.7-cm by 2.54-cm by 24.13-cm and positioned 1.27-cm in the Y-direction and 0-cm the other directions to create a cavity for the test plates. Just as the second block, the first block was subtracted by the third block. The fourth and fifth block were the test plates and had the dimensions 15.24-cm by 0.001-cm by 26.67-cm each and positioned 2.1844-cm in the Y-direction and 0-cm the other for block 4 and 0.6858-cm in the Y-direction for block 5. The first, fourth, and fifth blocks formed a union to simulate a clamping condition similar to the bolts on the payload. The design of the basic payload is shown below in Figure 10.

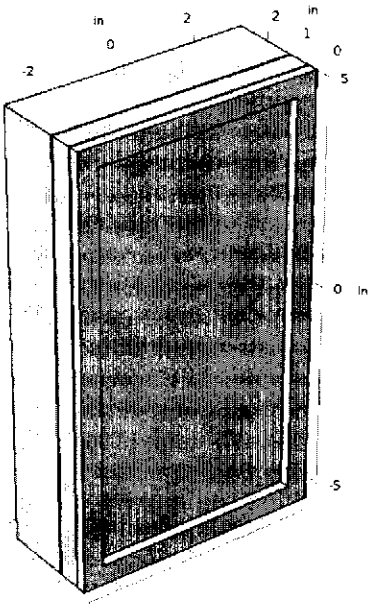

FIGURE 10: SIMPLIFIED MODEL OF THE PAYLOAD.

The model has all 4 sides of the top plate fixed and was subjected to gravitational accelerations shown in Figure 7, with longitudinal gravitational loading applied in the Z-direction dictated by the green arrow in Figure 8 and axial loads applied in the X-direction shown by the blue arrow in Figure 8 and Y-direction shown with a red arrow in Figure 8. From the Falcon 9 loading data the longitudinal acceleration ranged from -3Gs to 3Gs, and the axial accelerations ranged from -4Gs to 9Gs. In COMSOL this was modeled by creating variables that change the acceleration of the longitudinal and axial loadings to simulate the different loading conditions that the payload will undergo. To accomplish this in COMSOL a parametric sweep was created for a stationary study with the variables having a step size of 0.5.

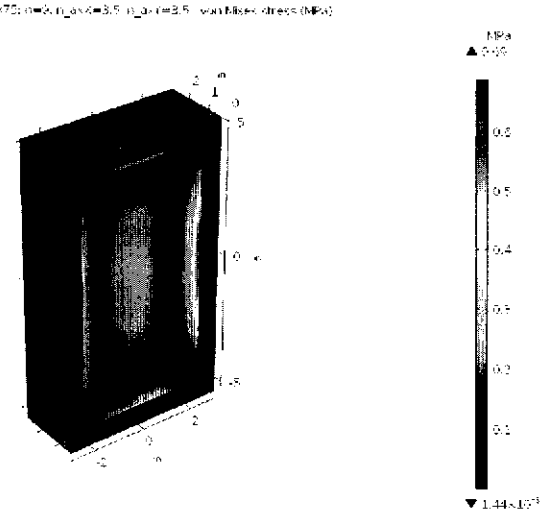

(a)

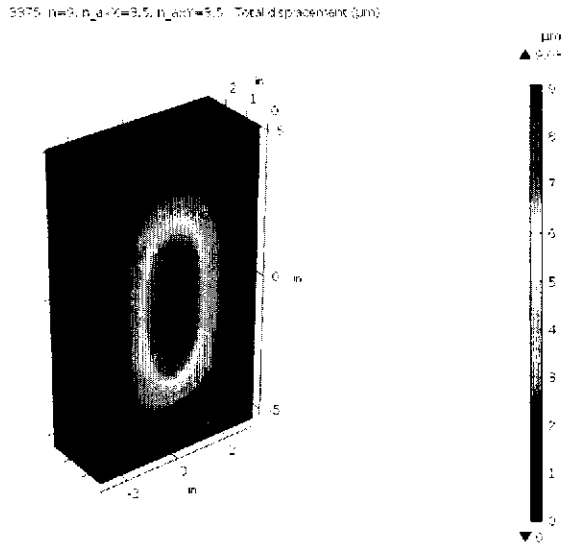

(b)

FIGURE 11: COMSOL ANALYSIS WITH ACCELERATION APPLIED TO SURFACE, SHORT-SIDE, AND LONG-SIDE. (a) STRESS RESULTS (b) DISPLACEMENT RESULTS.

The results show that the maximum stress is about 0.69 MPa as shown in Figure 11a and the maximum displacement is 9.08 μm as shown by Figure 11b. Since this is the maximum possible stress that the payload may endure this gives us a safety factor of 99,855 which shows that the payload will undoubtedly survive the launch with no chance of warping. These values occur when the variable n is equal to 9 and variables n_{axX} and n_{axY} are equal to 3. Variable n correlates to the longitudinal acceleration in the Z-direction and variables n_{axX} and n_{axY} correspond to axial acceleration in the X-direction and Y-direction, respectively. Most of the stress occurs around the edges of the test plates; this stress is due to a moment of the weight of the plate itself when at high gravitational loads. The maximum displacement occurs at the center of the test plates, and due to the small displacement, there is no concern about the plates warping and causing the piezoelectric sensors to detect irregular data.

5.4. Thermal Characteristics of Payload during Operation in LEO Environment

5.4.1. Development of Artificial Modeling Environment

The thermal environment was simulated in COMSOL 5.3 by including three different heat fluxes, and a heat rate. During these simulations, an ambient temperature of 25°C was assumed to analyze the thermal gradient of the payload. Analyzing the thermal gradient is critical, it will determine how the electrical hardware and heat fluxes will transfer heat within the payload, and the payload survivability during thermal fluctuations. As mentioned earlier, thermal radiation is the only heat transfer taking place so there will be no conduction or convection. Therefore, the three heat fluxes: solar, infrared (the Earth and ISS), and Albedo were provided by [11], where the average heat flux on Alpha Magnetic Spectrometer main radiators, orientated in the WAKE region were plotted with respect to Beta angle. The solar flux value was chosen for the simulation expected the payload to experience the maximum amount of heat flux. The infrared heat fluxes are the summation of the infrared coming from Earth and ISS components. The Albedo heat flux was a constant value of 15.46 W/m^2. The value for solar flux was chosen at 367 W/m^2, and the infrared flux was a constant value at 114 W/m^2. A heat rate of 7 W is the given output of the MD7 hardware [16,18,19].

5.4.2 Thermal Gradient Applied to Payload

A three-dimensional heat transfer of solids study was selected as the basic study in COMSOL 5.3. A fine mesh setting was established, with element sizes ranging from 2.67-mm to 21.3-mm at an element growth rate of 1.45, and a curvature factor of 0.5. The previously-mentioned simplified geometry payload was imported and used to avoid over-constraining the model from sources such as the heat sink. The arrows, shown in Figure 12c, illustrate the direction of heat fluxes and the heat rate of the MD7 hardware. The heat flux radiates into the payload through the top plate, and an output heat rate radiates from the payload. All boundaries are fixed except for the top face of the top plate and the top plate cover as

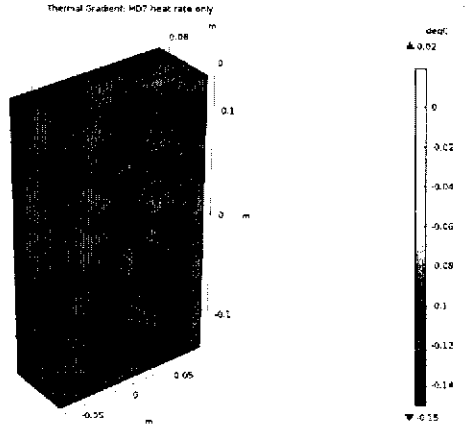

(a)

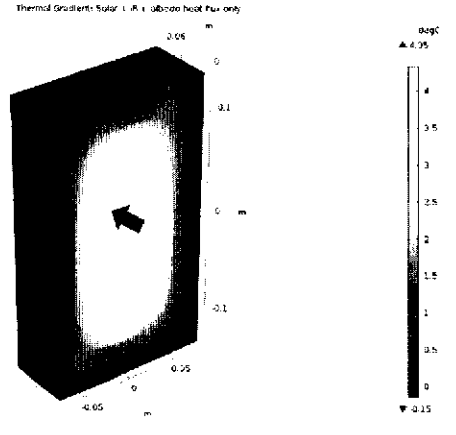

(b)

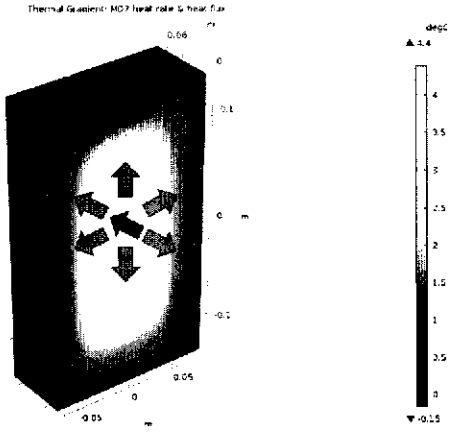

(c)

FIGURE 12: THERMAL GRADIENT OF PAYLOAD (a) MD7 HARDWARE HEAT RATE ONLY (b) HEAT FLUX ONLY (c) HEAT RATE AND HEAT FLUX

the combined surface area absorbs the heat fluxes and facilitates an output heat flow and maintains the optimal operational thermal window ranging from -18°C to 60°C while attached to the MISSE-12 platform. A room temperature boundary was added to the base; heat fluxes and heat rate were applied separately and jointly as seen in Figure 12 to the top plate and top frame to simulate the behavior of the throughout the payload during operation on the exterior of the ISS. Additionally, it was imperative to establish a room temperature boundary in the model to distinguish between thermal gradients and heat fluxes.

The finite-element studies revealed that the payload experiences an increase in temperature of 0.02°C, seen in Figure 12a, while the ambient temperature is room temperature (i.e., 298K or 25°C) and a heat rate of 5W representative of the heat emitted from the MD7 system. A summation of the heat fluxes depicted in Figure 12b shows a significant increase of 4.35°C as the heat fluxes are aligned normal to the face of the top plate.

The next study combined the heat rate and flux, yielding an increase of 4.4°C as seen in Figure 12c. The main concern is that heat fluxes will heat the payload more than the MD7 hardware as the heat fluxes have a more significant impact on the payload than the MD7 hardware.

6. CONCLUSION

The ISS payload design has been optimized to the standards and requirements given to the team by Alpha Space Test & Research Alliance, LLC, the payload integrator. The payload that will house the SHM experiments has been designed to be resilient to the extremes of the LEO. The data from the completed finite element analysis provides guidelines regarding what should be expected from the payload while in orbit installed on the International Space Station.

ACKNOWLEDGMENTS

The IOSHM team would like to acknowledge NASA Johnson Space Center for providing funding for this project through the NASA EpSCoR ISS program. Additionally, IOSHM would like to thank John Sanchez, a graduate student at the New Mexico Institute of Mining and Technology, for developing experimental data acquisition techniques, and David Hunter for providing test equipment. IOSHM would also like to acknowledge the invaluable work done by Luke Byrom, Shane McKinney, and Michael Underwood as the project has progressed.

REFERENCES

[1] Tandon, A., Byrom, L., Bancroft, C., MacNinch, D., Mckinney, S., Pacheco, D., Underwood, M, and Zagrai, A., 2019. "Payload Design and Development for Orbital Structural Health Monitoring," New Mexico Institute of Mining and Technology, Socorro, NM.

[2] Baumann, E.W., Becker, R.S., Ellerbrock, P.J. and Jacobs, S.W., (1997), "DC-XA structural health monitoring system," Proceedings of SPIE's Smart Structures and Materials, Vol. 3044, pp. 195–206.

[3] Finlayson, R.D., Schaafsma, D.T., Shen, H.W., Carlos, M.F., Miller, R.K., and Shepherd, B., (2001), "Continuous health monitoring of Graphite Epoxy Motorcases (GEM)," Proceedings of SPIE's Smart Structures and Materials, Vol. 4335, pp. 155-166.

[4] Kabashima, S., Ozaki, T., Takeda, N., (2001), "Structural health Monitoring using FBG Sensor in Space Environment," Proceedings of SPIE, Vol. 4332, pp. 78-87.

[5] Mckenzie, I. and Karafolas, N., (2005), "Fiber optic sensing in space structures: the experience of the European Space Agency," Proceedings of SPIE, Vol. 5855, pp. 262-269.

[6] Güemes, A., Fernández-López, A., Díaz-Maroto, P.F., Lozano, A., Sierra-Perez, J., (2018) "Structural Health Monitoring in Composite Structures by Fiber-Optic Sensors," *Sensors* 2018, 18, 1094; doi:10.3390/s18041094

[7] Boller, C., Chang, F.-K., Fujino, Y., (2009), (editors), "Encyclopedia of Structural Health Monitoring," Wiley.

[8] Giurgiutiu, V. *Structural Health Monitoring with Piezoelectric Wafer Active Sensors*, 2nd edition, Academic Press, 2014.

[9] Michaels, J.E., 2008, "Ultrasonic structural health monitoring: Strategies, issues and progress.:, Proceedings of SPIE - The International Society for Optical Engineering. 6933. 10.1117/12.778700., pp.1.

[10] Qing X.P., Chan H.L., Beard S.J., and Kumar, A., (2006), "An active diagnostic system for structural health monitoring of rocket engines," J. Intell. Mater. Syst. Struct. Vol. 17, pp. 619–628.

[11] Yu, P., (2007), "Real-time Impact Detection System for Thermal Protection System," Proceedings of 6th International Workshop on Structural Health Monitoring, Stanford, (2007), Vol. 1, pp. 153-158.
[12] Cuc, A., Giurgiutiu, V., Joshi, S., and Tidwell, Z., (2007), "Structural Health Monitoring with Piezoelectric Wafer Active Sensors for Space Applications," AIAA Journal, Vol. 45, No. 12, December, (2007).
[13] Zagrai, A., Doyle, D., Gigineishvili, V., Brown, J., Gardenier, H., Arritt, B., (2010) "Piezoelectric Wafer Active Sensor Structural Health Monitoring of Space Structures," Journal of Intelligent Material Systems and Structures, Vol. 21, N. 9, pp. 921-940, first published on May 4, 2010.
[14] Zagrai, A, (2011) "Piezoelectric Wafer Active Sensing During Suborbital Space Flight," Technical presentation at ASME Conference on Smart Materials, Adaptive Structures and Intelligent Systems, September 18 – 21, 2011, Scottsdale, AZ, presentation: SMASIS2011-5274.
[15] Zagrai, A.N., Demidovich, N., Cooper, B., Schlavin, J., White, C., Kessler S., MacGillivray, J., Chesebrough, S., Magnusion, L., Puckett, L., Tena, K., Gutierrez, J., Trujillo, B., Siler, D., Gonzales, T., (2015) "Structural Health Monitoring during Suborbital Spaceflight," Proceedings of 66th International Astronautical Congress, 12-16 October 2015, Jerusalem, Israel, IAC-15,C2,5,3,x29660.
[16] Shabany, Y., 2008, "Simplified Correlations For Radiation Heat Transfer Rate ...," *Electronics Cooling*, [Online]. Available: https://www.electronics-cooling.com/2008/08/simplified-correlations-for-radiation-heat-transfer-rate-in-plate-fin-heat-sinks/. [Accessed: 4-Apr-2019].
[17] Meseguer, J., Pérez-Grande, I., Sanz-Andrés, A. "Spacecraft Thermal Control", Woodhead Publishing, 2012.
[18] Chisibas, R.S.S., Loureiro, G., and de Oliveira Lino, C., 2018. "Space Thermal and Vacuum Environment Simulation", National Institute for Space Research, INPE, São Paulo, Brazil.
[19] Xie, M., Gao, J., Wu, S., and Qin, Y., 2016. "Thermal conditions on the International Space Station: Heat flux and temperature investigation of main radiators for the Alpha Magnetic Spectrometer", School of Energy Science and Engineering, Harbin Institute of Technology, Harbin 150001, China.
[20] Cihan, M., Haktanır, O.O., Akbulut, I., and Aslan. A. R., 2014. "Flight Dynamic Analysis of ITUpSAT1", İstanbul Technical University, Faculty of Aeronautics and Astronautics, Dept of Space Engineering.
[21] Navid Namdari, N., and Dehghan, A., 2018. "Natural frequencies and mode shapes for vibrations of rectangular and circular membranes: A numerical study," International Research Journal of Advanced Engineering and Science, Volume 3, Issue 2, pp. 30-34.
[22] Space Exploration Technologies Corp. (SpaceX), 2019, 'Falcon's User Guide".
[23] Farrell, L. (2019). *MISSE-12 Kickoff.* Alpha Space Test & Research Alliance, LLC
[24] Wickramatunga, R., "United Nations Office for Outer Space Affairs," *United Nations Register of Objects Launched into Outer Space.* [Online]. Available: http://www.unoosa.org/oosa/en/spaceobjectregister/index.html. [Accessed: 20-Apr-2019].

NEW MEXICO TECH
SCIENCE • ENGINEERING • RESEARCH • UNIVERSITY

Application for Senate Bills

Requesting Club/Agency: _____

Classification: ☐ SGA Club ☐ Associate Club ☐ Sports Club ☒ Other

If an SGA club, what were your required volunteer hours (last semester): _____

How many hours has your club fulfilled to date: _____

Please detail events where volunteer credit was earned:

_____

_____

Requested Amount of funding: $ 1200.00

Event: Imecc 2019 Conference

Location: Salt Lake City Utah

Event Dates: November 11th - 14th 2019

Have you received funding from another source for this event: ☐ Yes ☒ No

If yes, how much: _____

From whom: _____

Have you fundraised for this event? ☐ Yes ☒ No

If yes, please detail the fundraiser and how much money was earned. _____

_____

_____

If requesting funds for traveling please fill out below information:

Members Attending: Undergraduate: 1 Graduate: _____ Special: _____

Method of Travel: ☐ NMT Vehicle ☐ Personal Vehicle ☒ Plane ☐ Other

FOR ALL REQUESTING AGENCIES:

Please attach a ONE PAGE (12 pt. font) explanation for your funding request. This should include any additional information relevant to your request and an itemized budget with exact costs and explanations for all necessary items which may or may not include: Supplies and Materials, Services, Equipment, Travel, Registration, Etc.

Event/Project IMECE 2019 Conference Date of Event/Project 11/11/19 - 11/14/19

Group/Club IOSHM Design Team Department/Club Advisor Dr. Zagrai

Have you received funding from SUR for any other activities? ☐ No ☐ Yes:

APPLICANT'S INFORMATION

Name Douglas L. MacNinch ID 900330127 ☑Undergraduate ☐ Graduate

Email douglas.macninch@student.nmt.edu Cell 505-228-5033

Names of student(s) being funded (attach additional sheet if necessary):

Funding from SGA or other offices? ☒ No ☐ Yes - *office(s) and amount(s) below*

_____ $_____ / _____ $_____ / _____ $_____

INSTRUCTIONS: Itemize all budget elements and attach quotations from vendors and/or an additional page justifying how you arrived at the cost. You may be asked to submit additional information.

Travel _____ Total _____

Registration _____ Total _____

Supplies and Materials _____ Total _____

Other _____ Total _____

Grand Total

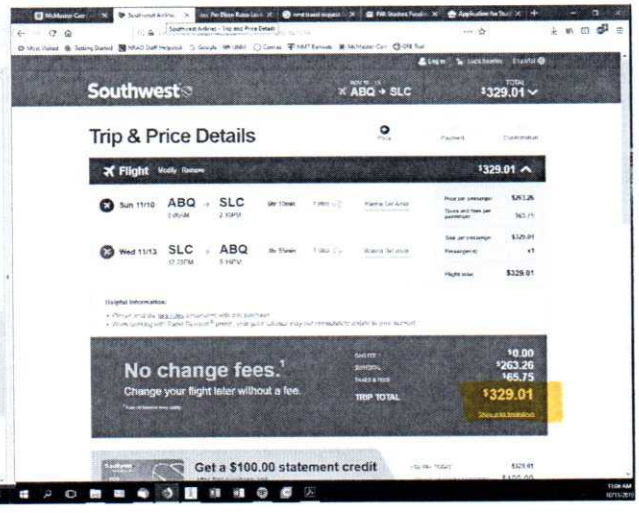

Event/Project IMECE 2019 Conference Date of Event/Project 11/11/19 - 11/14/19

Group/Club IOSHM Design Team Department/Club Advisor Dr. Zagrai

Have you received funding from SUR for any other activities? ☐ No ☐ Yes:

APPLICANT'S INFORMATION

Name Douglas L. MacNinch ID 900330127 ☑Undergraduate ☐ Graduate

Email douglas.macninch@student.nmt.edu Cell 505-228-5033

Names of student(s) being funded (attach additional sheet if necessary):

Funding from SGA or other offices? ☒ No ☐ Yes - *office(s) and amount(s) below*

_____ $_____ / _____ $_____ / _____ $_____

INSTRUCTIONS: Itemize all budget elements and attach quotations from vendors and/or an additional page justifying how you arrived at the cost. You may be asked to submit additional information.

Travel Flight $329.01, Total _____

Registration _____ Total _____

Supplies and Materials _____ Total _____

Other _____ Total _____

Grand Total

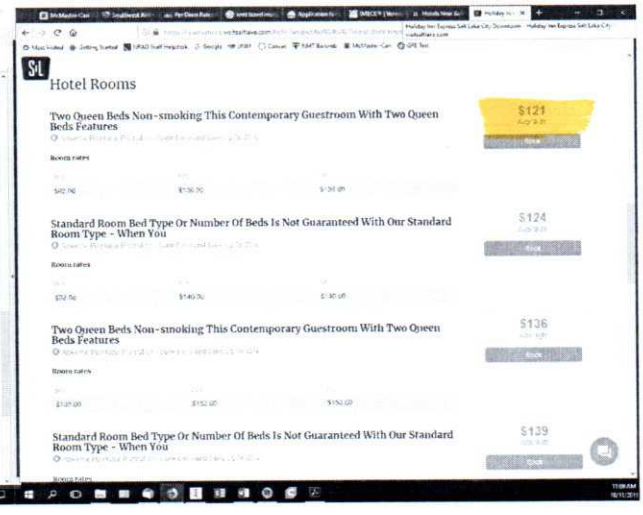

Event/Project IMECE 2019 Conference Date of Event/Project 11/11/19 - 11/14/19

Group/Club IOSHM Design Team Department/Club Advisor Dr. Zagrai

Have you received funding from SUR for any other activities? ☐ No ☐ Yes:

APPLICANT'S INFORMATION

Name Douglas L. MacNinch ID 900330127 ☑Undergraduate ☐ Graduate

Email douglas.macninch@student.nmt.edu Cell 505-228-5033

Names of student(s) being funded (attach additional sheet if necessary):

Funding from SGA or other offices? ☒ No ☐ Yes - *office(s) and amount(s) below*

_____ $_____ / _____ $_____ / _____ $_____

INSTRUCTIONS: Itemize all budget elements and attach quotations from vendors and/or an additional page justifying how you arrived at the cost. You may be asked to submit additional information.

Travel Flight $329.01, Total _____

Registration _____ Total _____

Supplies and Materials _____ Total _____

Other _____ Total _____

Grand Total

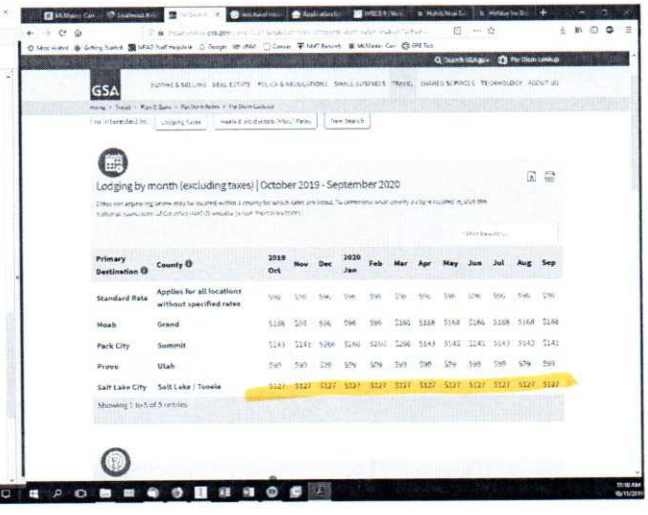

NEW MEXICO TECH
SCIENCE • ENGINEERING • RESEARCH • UNIVERSITY

Travel Funding Request

Budget Item	Total
Transportation	329.01
Lodging/Meals	508.00+365.00
Registration/Misc.	

Grand Total: 1200.01

Transportation (Vans, Gas, Flights, Rentals, Taxis)			
Items: Highest to Lowest Priority	Quantity	Price Each	Total
		Total:	

Lodging/Meals			
Items: Highest to Lowest Priority	Quantity	Price Each	Total
		Total:	

Registration/Miscellaneous			
Items: Highest to Lowest Priority	Quantity	Price Each	Total
		Total:	